

Expansion of the tetragonal magnetic phase with pressure in the iron-arsenide superconductor $\text{Ba}_{1-x}\text{K}_x\text{Fe}_2\text{As}_2$

E. Hassinger,^{1,*} G. Gredat,¹ F. Valade,¹ S. René de Cotret,¹ O. Cyr-Choinière,¹ A. Juneau-Fecteau,¹ J.-Ph. Reid,¹ H. Kim,² M. A. Tanatar,² R. Prozorov,^{2,3} B. Shen,⁴ H.-H. Wen,^{4,5} N. Doiron-Leyraud,¹ and Louis Taillefer^{1,5,†}

¹*Département de physique & RQMP, Université de Sherbrooke, Sherbrooke, Québec J1K 2R1, Canada*

²*Ames Laboratory, Ames, Iowa 50011, USA*

³*Department of Physics and Astronomy, Iowa State University, Ames, Iowa 50011, USA*

⁴*Center for Superconducting Physics and Materials,*

National Laboratory of Solid State Microstructures and Department of Physics, Nanjing University, Nanjing 210093, China

⁵*Canadian Institute for Advanced Research, Toronto, Ontario M5G 1Z8, Canada*

(Dated: December 21, 2015)

In the temperature-concentration phase diagram of most iron-based superconductors, antiferromagnetic order is gradually suppressed to zero at a critical point, and a dome of superconductivity forms around that point. The nature of the magnetic phase and its fluctuations is of fundamental importance for elucidating the pairing mechanism. In $\text{Ba}_{1-x}\text{K}_x\text{Fe}_2\text{As}_2$ and $\text{Ba}_{1-x}\text{Na}_x\text{Fe}_2\text{As}_2$, it has recently become clear that the usual stripe-like magnetic phase, of orthorhombic symmetry, gives way to a second magnetic phase, of tetragonal symmetry, near the critical point, between $x = 0.24$ and $x = 0.28$. Here we report measurements of the electrical resistivity of $\text{Ba}_{1-x}\text{K}_x\text{Fe}_2\text{As}_2$ under applied hydrostatic pressures up to 2.75 GPa, for $x = 0.22, 0.24$ and 0.28 . We track the onset of the tetragonal magnetic phase using the sharp anomaly it produces in the resistivity. In the temperature-concentration phase diagram of $\text{Ba}_{1-x}\text{K}_x\text{Fe}_2\text{As}_2$, we find that pressure greatly expands the tetragonal magnetic phase, while the stripe-like phase shrinks. This raises the interesting possibility that the fluctuations of the former phase might be involved in the pairing mechanism responsible for the superconductivity.

PACS numbers: 74.25.Fy, 74.70.Dd

The phase diagram of iron-based superconductors of the BaFe_2As_2 family is characterized by competing antiferromagnetic (AF) order and superconductivity. Usually, the AF order decreases with concentration (doping) and a dome of superconductivity surrounds the critical point.¹ The AF order is a stripe-like spin-density wave, with a wavevector $\mathbf{Q} = (\pi, 0)$ and the magnetic moments lie in the plane. At the magnetic transition temperature, or slightly above it, the lattice changes from tetragonal at high temperature to orthorhombic at low temperature.^{2,3}

In $\text{Ba}_{1-x}\text{X}_x\text{Fe}_2\text{As}_2$, where $\text{X} = \text{K}$ or Na , the phase diagram was recently found to be richer than this simple picture. Resistivity measurements under pressure revealed the existence of an internal transition inside the AF phase of $\text{Ba}_{1-x}\text{K}_x\text{Fe}_2\text{As}_2$.⁴ As the onset temperature T_N of the orthorhombic AF phase (o-AF) is suppressed with hydrostatic pressure P , an additional phase transition to a “new phase” appears below a transition temperature $T_0 < T_N$, for $0.16 < x < 0.21$, when $P > 0.9$ GPa.⁴ A tetragonal magnetic phase (t-AF) was then discovered in the closely related compound $\text{Ba}_{1-x}\text{Na}_x\text{Fe}_2\text{As}_2$, for $0.24 < x < 0.28$, by neutron and x-ray diffraction on powder samples.⁵ Subsequent neutron scattering on single crystals showed that in this t-AF phase the spins are aligned parallel to the c axis.⁶ A similar phase of tetragonal symmetry was then found in $\text{Ba}_{1-x}\text{K}_x\text{Fe}_2\text{As}_2$ at ambient pressure, for $0.24 < x < 0.28$.⁷ The magnetic moments in the t-AF phase of $\text{Ba}_{1-x}\text{K}_x\text{Fe}_2\text{As}_2$ are also oriented along the c axis.^{8,9} Infrared spectroscopy showed that the t-AF phase has a double- Q magnetic structure,⁸

as opposed to the single- Q structure of the o-AF phase. Several theoretical studies have investigated the properties of the tetragonal magnetic phase in iron-based superconductors.^{5,10–19}

In this Article, we extend our prior study of $\text{Ba}_{1-x}\text{K}_x\text{Fe}_2\text{As}_2$ under pressure, performed up to $x = 0.21$,⁴ by studying three further samples, with $x = 0.22, 0.24$ and 0.28 . We are able to connect the additional phase induced by pressure with the tetragonal phase seen at ambient pressure. Pressure is seen to cause a dramatic expansion of the tetragonal magnetic phase, on the backdrop of a shrinking orthorhombic phase.

Methods.— Single crystals of $\text{Ba}_{1-x}\text{K}_x\text{Fe}_2\text{As}_2$ were grown from self flux.²⁰ Three underdoped samples were measured, with a superconducting transition temperature $T_c = 20.8 \pm 0.5$ K, 25.4 ± 0.5 K, and 30.1 ± 0.5 K, respectively. Using the relation between T_c and the nominal K concentration x reported in ref. 3 and wavelength-dispersive x-ray spectroscopy,²¹ we obtain $x = 0.22, 0.24$ and 0.28 , respectively. These x values are also consistent with the measured antiferromagnetic ordering temperature T_N (which coincides with the structural transition from tetragonal to orthorhombic),³ equal to 91 ± 5 K and 79 ± 2 K, respectively for the two lower dopings. The sample with $x = 0.28$ shows no magnetic or structural transition. The resistivity at room temperature of all samples lies between 250 and 350 $\mu\Omega$ cm, in agreement with previous studies.²² As before,⁴ we have normalized the resistivity at $T = 300$ K to 300 $\mu\Omega$ cm. Hydrostatic pressures up to 2.75 GPa were applied with a

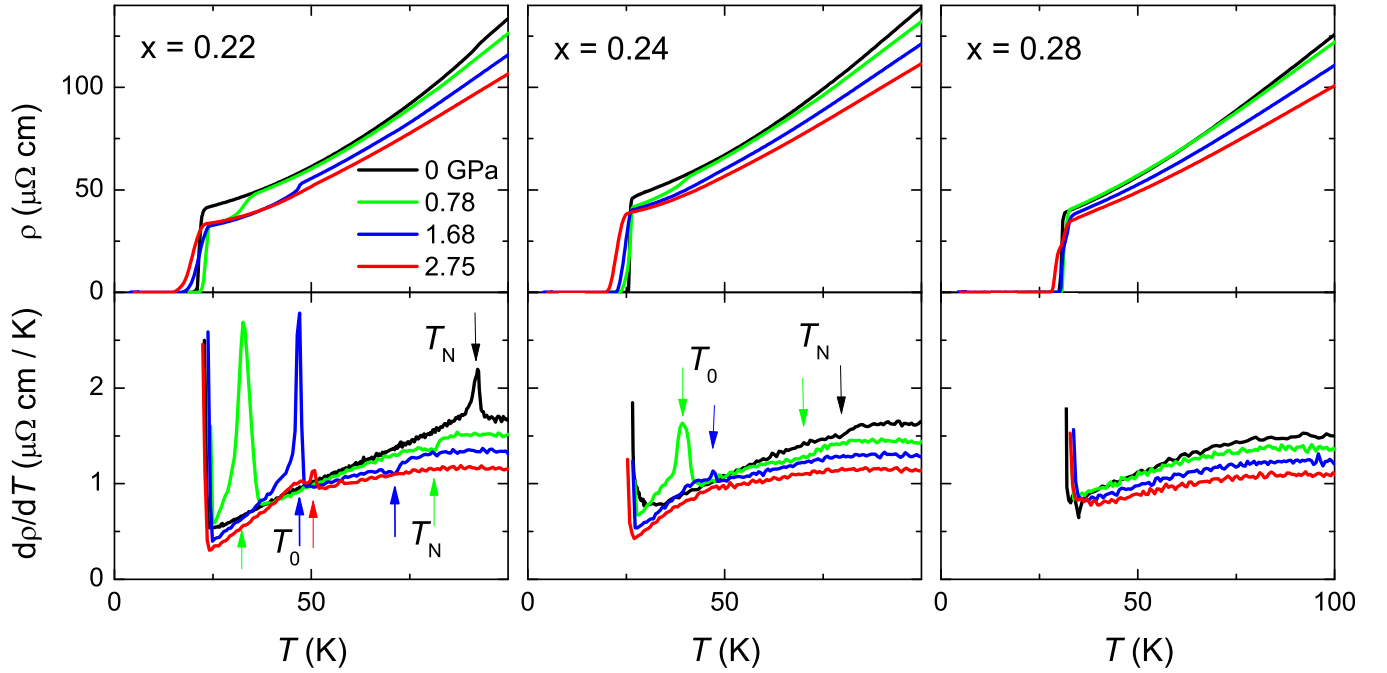


FIG. 1: *Top*: In-plane electrical resistivity of $\text{Ba}_{1-x}\text{K}_x\text{Fe}_2\text{As}_2$ for $x = 0.22$, $x = 0.24$ and $x = 0.28$ (different columns) for four different pressures, as indicated. *Bottom*: Temperature derivative of the data in the top panels. The peak (dip) between 60 K and 100 K signals the onset of stripe-like antiferromagnetic order at T_N (arrows). The peak at lower temperature signals the onset of the tetragonal magnetic phase at T_0 (arrows).

hybrid piston-cylinder cell,²³ using a 50:50 mixture of n-pentane:isopentane.²⁴ The pressure was measured via the superconducting transition of a lead wire inside the pressure cell. The electrical resistivity ρ was measured for a current in the basal plane of the orthorhombic crystal structure, with a standard four-point technique using a Lakeshore ac-resistance bridge. The transition temperatures are defined as follows: T_c is where $\rho = 0$; T_N and T_0 are detected as extrema in the derivative $d\rho/dT$.

Resistivity.— Fig. 1 shows the in-plane resistivity (top panels) and its temperature derivative (bottom panels) of each sample, for a selection of pressures. T_N is detected as a peak in the derivative for the first sample at ambient pressure, and then as a dip for higher pressures or doping. The transition at T_0 shows up as a sharp peak, below T_N . In Fig. 2, the full set of derivative curves is displayed for $x = 0.22$ and $x = 0.24$, allowing to track the anomalies at T_N and T_0 as a function of pressure.

As previously reported for samples with lower doping,⁴ T_N decreases linearly with pressure. For $x = 0.22$, the peak in the derivative at T_N evolves into a dip at 0.48 GPa. We are able to follow this dip up to $P = 2$ GPa, above which it disappears. The evolution of the peak at T_0 is different. At 0.48 GPa, the peak at T_0 appears. T_0 goes up with pressure until it stays almost constant above 2.3 GPa. The height of the sharp peak at T_0 increases slightly at first, and then decreases above $P \simeq 1.5$ GPa. The behavior for $x = 0.24$ is similar, but shifted to lower pressures. T_N can be followed only up to 0.94 GPa. The transition at T_0 appears as a peak as

soon as we apply pressure. In fact, a slight upturn of the derivative with decreasing T , indicative of an onset of the transition at T_0 , can be seen even at ambient pressure. The peak at T_0 stays sharp but its height decreases above $P \simeq 1$ GPa, and the last pressure where it is observed is 1.68 GPa. The curve at this pressure looks very much like the one at the highest pressure in the $x = 0.22$ sample.

Temperature-pressure phase diagram.— Fig. 3 presents the temperature-pressure phase diagram for the three samples. T_N decreases linearly with P , with a slightly steeper slope at $x = 0.24$. By contrast, T_0 rises rapidly, at least initially. At $x = 0.22$, T_0 saturates above $P = 2.3$ GPa. At $x = 0.24$, we can no longer detect T_0 above $P = 1.68$ GPa (Fig. 2), the pressure at which it merges with the T_0 line at $x = 0.22$ (Fig. 3).

At $x = 0.24$, the phase diagram is such that if the T_0 line (blue) saturates at high pressure as it does in the case of $x = 0.22$ (red T_0 line), then a linear extension of the T_N line (blue) will hit that T_0 line, implying that the t-AF phase would persist to pressures beyond the end of the o-AF phase.

As for superconductivity, note that T_c decreases as soon as the tetragonal phase appears (Fig. 3), as found in prior studies of $\text{Ba}_{1-x}\text{K}_x\text{Fe}_2\text{As}_2$ (refs. 4,26) and $\text{Ba}_{1-x}\text{Na}_x\text{Fe}_2\text{As}_2$,^{25,26} in agreement with the negative dT_c/dP expected from the Ehrenfest relation applied to the thermodynamic data.⁷

Temperature-concentration phase diagram.— Combining our present results with those of our previous study,⁴ we plot the temperature-concentration phase diagram of

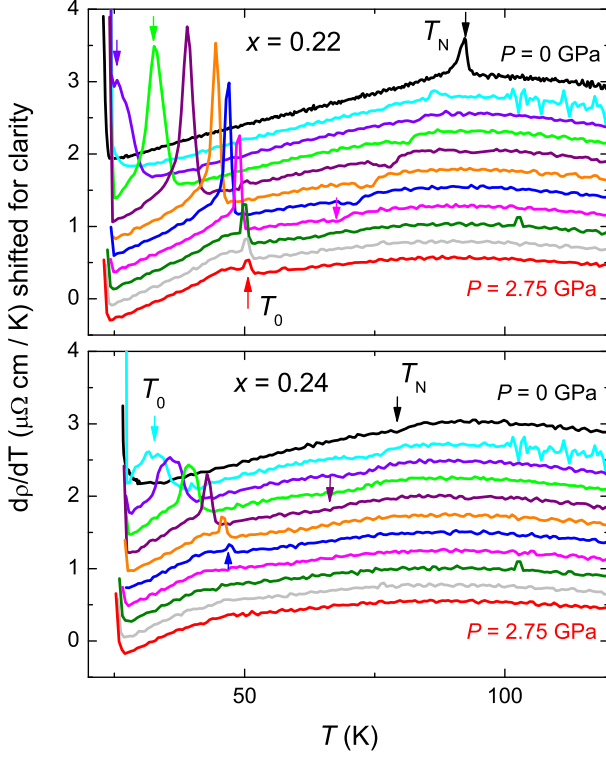


FIG. 2: *Top*: Temperature derivative of the resistivity of $\text{Ba}_{1-x}\text{K}_x\text{Fe}_2\text{As}_2$ with $x = 0.22$, for 11 different pressures, from ambient pressure ($P = 0$) at the top (black) to $P = 2.75$ GPa at the bottom (red), with the following intermediate values: $P = 0.28, 0.48, 0.78, 0.94, 1.37, 1.68, 2.0, 2.31$, and 2.4 GPa. The curves are shifted for clarity. The black down-pointing arrow marks T_N at $P = 0$. The next down-pointing arrow marks T_N at the highest pressure where it can still be detected. T_0 shows up as a peak at low temperature. The up-pointing arrows mark T_0 at the highest pressure where the peak can still be detected. *Bottom*: The same for $x = 0.24$.

$\text{Ba}_{1-x}\text{K}_x\text{Fe}_2\text{As}_2$ in Fig. 4. For comparison, we also reproduce the phase diagram at zero pressure reported in ref. 7; the agreement with our own ambient-pressure data is excellent. We see that the T_N line moves down with pressure, in parallel fashion. This suggests that the critical concentration x_N where T_N goes to zero shifts down with pressure.

On the backdrop of this shrinking o-AF phase, the tetragonal magnetic phase undergoes a major expansion with pressure (Fig. 4). While the t-AF phase occupies a small area below T_N at ambient pressure, its area grows by an order of magnitude at $P = 2.4$ GPa. In other words, at high pressure the tetragonal phase becomes the dominant magnetic phase in the temperature-concentration phase diagram of $\text{Ba}_{1-x}\text{K}_x\text{Fe}_2\text{As}_2$. In the context of recent calculations, it may be that pressure favours the t-AF phase because it changes the ellipticity of the electron pockets in the Fermi surface of $\text{Ba}_{1-x}\text{K}_x\text{Fe}_2\text{As}_2$.¹⁵

Summary. – In summary, we have shown that the new phase discovered in $\text{Ba}_{1-x}\text{K}_x\text{Fe}_2\text{As}_2$ from sharp signatures in the resistivity under pressure⁴ is the tetragonal antiferromagnetic phase observed and identified subsequently by various probes in both $\text{Ba}_{1-x}\text{Na}_x\text{Fe}_2\text{As}_2$ (refs. 5,6) and $\text{Ba}_{1-x}\text{K}_x\text{Fe}_2\text{As}_2$.^{7–9} Under pressure, this t-AF phase expands enormously, by an order of magnitude for 2.4 GPa in terms of the area it occupies in the temperature-concentration phase diagram, relative to the orthorhombic stripe-like AF phase that dominates at ambient pressure. As a result, at high pressure superconductivity exists on the border of a dominant tetragonal magnetic phase. It is then likely that fluctuations of that double- Q phase play a role in the pairing. Recent calculations suggest that such fluctuations could actually enhance T_c .¹⁸

The work at Sherbrooke was supported by a Canada Research Chair, the Canadian Institute for Advanced Research, the National Science and Engineering Research Council of Canada, the Fonds de recherche du Québec - Nature et Technologies, and the Canada Foundation for Innovation. The work at the Ames Laboratory was supported by the DOE-Basic Energy Sciences under Contract No. DE-AC02-07CH11358. The work in China was supported by NSFC and the MOST of China (#2011CBA00100).

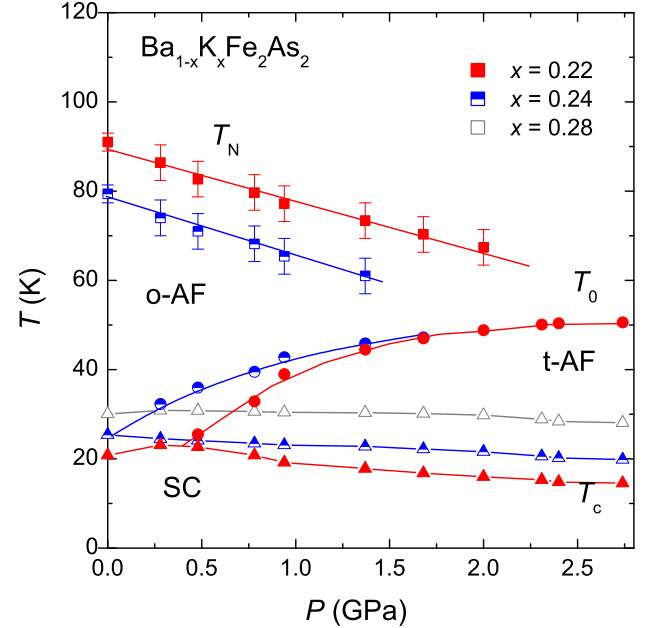


FIG. 3: Temperature-pressure phase diagram of $\text{Ba}_{1-x}\text{K}_x\text{Fe}_2\text{As}_2$, for $x = 0.22, 0.24$ and 0.28 (full, half-full and empty symbols, respectively), showing the orthorhombic antiferromagnetic (o-AF) transition temperature T_N (squares), the superconducting (SC) transition temperature T_c (triangles), and the tetragonal antiferromagnetic (t-AF) transition temperature T_0 (circles).

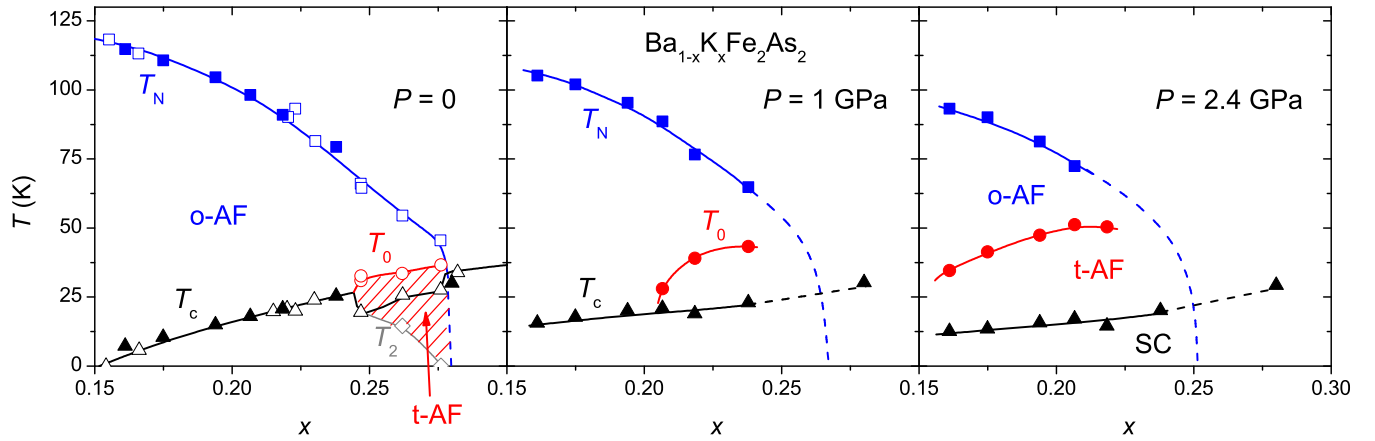


FIG. 4: Temperature-concentration phase diagram of $\text{Ba}_{1-x}\text{K}_x\text{Fe}_2\text{As}_2$, showing T_N (blue squares), T_0 (red circles) and T_c (black triangles), for three different values of the applied pressure: $P = 0$ (left panel), 1.0 GPa (middle panel) and 2.4 GPa (right panel). This includes data from our previous study.⁴ Ambient-pressure data from ref. 7 are also shown in the left panel (open symbols), including a transition back to the o-AF phase, below T_2 (diamonds). All lines are a guide to the eye. The evolution from left to right, with increasing pressure, reveals a major expansion of the tetragonal magnetic phase (t-AF), on the backdrop of a shrinking stripe phase (o-AF). Extrapolating to higher pressure, we expect the former to become the dominant magnetic phase coexisting with superconductivity in $\text{Ba}_{1-x}\text{K}_x\text{Fe}_2\text{As}_2$.

-
- * Electronic address: elena.hassinger@usherbrooke.ca
† Electronic address: louis.taillefer@usherbrooke.ca
- ¹ P. C. Canfield and S. L. Bud'ko, *Annu. Rev. Condens. Matter Phys.* **1**, 27 (2010).
 - ² D. K. Pratt *et al.*, *Phys. Rev. Lett.* **103**, 087001 (2009).
 - ³ S. Avci *et al.*, *Phys. Rev. B* **85**, 184507 (2012).
 - ⁴ E. Hassinger *et al.*, *Phys. Rev. B* **86**, 140502(R) (2012).
 - ⁵ S. Avci *et al.*, *Nat. Commun.* **5**, 3845 (2014).
 - ⁶ F. Waßer *et al.*, *Phys. Rev. B* **91**, 060505 (2015).
 - ⁷ A. Boehmer *et al.*, *Nat. Commun.* **6**, 7911 (2015).
 - ⁸ B. P. P. Mallet *et al.*, *Phys. Rev. Lett.* **115**, 027003 (2015).
 - ⁹ J. M. Allred *et al.*, *Phys. Rev. B* **92**, 094515 (2015).
 - ¹⁰ J. Lorenzana *et al.*, *Phys. Rev. Lett.* **101**, 186402 (2008).
 - ¹¹ I. Eremin and A. V. Chubukov, *Phys. Rev. B* **81**, 024511 (2010).
 - ¹² E. Berg *et al.*, *Phys. Rev. B* **81**, 172504 (2010).
 - ¹³ G. Giovannetti *et al.*, *Nat. Commun.* **2**, 398 (2011).
 - ¹⁴ P. M. R. Brydon *et al.*, *Phys. Rev. B* **84**, 214510 (2011).
 - ¹⁵ J. Wang *et al.*, *Phys. Rev. B* **91**, 121104 (2015).
 - ¹⁶ X. Kang *et al.*, *Phys. Rev. B* **91**, 024401 (2015).
 - ¹⁷ M. N. Gastiasoro *et al.*, arXiv:1502.05859 (2015).
 - ¹⁸ R. M. Fernandes *et al.*, arXiv:1504.03656 (2015).
 - ¹⁹ J. M. Allred *et al.*, arXiv:1505.06175 (2015).
 - ²⁰ H.-Q. Luo *et al.*, *Supercond. Sci. Technol.* **21**, 125014 (2008).
 - ²¹ M. Tanatar *et al.* *Phys. Rev. B* **89**, 144514 (2014).
 - ²² Y. Liu *et al.* *Phys. Rev. B* **89**, 134504 (2014).
 - ²³ I. R. Walker, *Rev. Sci. Instrum.* **70**, 3402 (1999).
 - ²⁴ W. J. Duncan *et al.*, *J. Phys.: Condens. Matter* **22**, 052201 (2010).
 - ²⁵ S. Bud'ko *et al.*, *Phys. Rev. B* **89**, 014510 (2014).
 - ²⁶ S. Bud'ko *et al.*, *Phys. Rev. B* **87**, 100509(R) (2013).